Symmetry, Radical Ions, and Butadienes: Exploring the Limits of Density Functional Theory

Jonas Oxgaard and Olaf Wiest*

Department of Chemistry and Biochemistry, University of Notre Dame, Notre Dame, Indiana 46556-5670

Received: April 10, 2001; In Final Form: June 11, 2001

Pure and hybrid density functional theory (DFT) methods are evaluated regarding their ability to correctly describe asymmetric transition structures for symmetric butadiene radical cations. The study covers unsubstituted butadiene radical cation as well as (2,3-X,X)-disubstituted butadiene radical cations, where X is -CH_3, -OH, -F, or -SiH_3. The DFT methods either converge toward an erroneous symmetric solution or describe the asymmetric transition structure qualitatively correctly. Whether or not the asymmetric transition structure is found depends on the amount of Hartree−Fock density exchange included in the method, as well as on the electronic characteristics of the substituents, as described by their σ^+ values. The disparate behaviors encountered are rationalized by a two-state model. It is also shown that molecular symmetry does not automatically induce errors, as reported by earlier studies. Instead, electronic symmetry is introduced as a factor to observe when organic radical cations are studied computationally.

1. Introduction

Recent years have seen the ascendance of density functional theory (DFT) as an efficient and affordable alternative to traditional post-Hartree−Fock (HF) methods.[1,2] Favorable scaling yields a computational cost comparable to a self-consistent field (SCF) calculation, with quality of results equaling a second-order Moller−Plesset (MP2) calculation in areas ranging from closed-shell geometries of molecules and transition states,[3] heats of formation,[4] spectroscopic properties,[5] and gas-phase acidities.[6] In areas requiring extensive electron correlation, such as structures involving transition metals[7] or open-shell species,[2] the results from DFT calculations are often in better agreement with the available experimental data and highly correlated molecular orbital (MO) calculations than HF or MP2 calculations. This makes them an attractive alternative to the very costly coupled cluster (CC) and quadratic configuration interaction (QCI) methods.

Nevertheless, DFT does have some problematic areas, perhaps most notably a tendency to overestimate delocalization. This bias is usually quite benign for neutral species, yielding energies of formation 1−2 kcal/mol too low, as compared to experiment.[8] In some cases, e.g., the ground-state geometry of styrene, this is enough to overcome a small steric influence and thus predict an erroneous planar geometry as the minimum energy conformer instead of the correct, slightly twisted gauche geometry.[9] However, as this problem is fairly well-defined, examining HF or MP2 geometries in systems where delocalization is expected to be a problem can usually compensate for this bias.

Unfortunately, this is not the case for radical ions and other open-shell species. Not only are ab initio alternatives unreliable[10] or expensive, but DFT also experiences some serious problems when confronted with delocalized radical ions. These problems, despite being known in principle for some time[11] as well as described in studies of $(H_2O)_2^{\bullet+}$,[12] ($HOOH^-$),[13] and (F_2^-),[14] were first characterized as a systematic failing of current DFT methods by Bally and co-workers in their study of acetylene dimer radical cation[15] and further explored by Bally and Sastry in their study of the dissociation of $(H_2)^{\bullet+}$ and $(He_2)^{\bullet+}$.[16] In the latter study, they found that DFT overestimated the energy of dissociation by 5.3 and 29.0 kcal/mol, respectively, and that while utilizing hybrid methods reduced the magnitude of the error, even the BHandHLYP method, which incorporates a 50% admixture of HF exchange density, produced errors of 2.3 and 12.4 kcal/mol, respectively. Further examination revealed that DFT failed to localize the spin and charge for the dissociated atoms even at large distances. The authors concluded that DFT failed to correctly describe localization of spin and charge in symmetrical radical ions, something they aptly labeled inverse symmetry breaking.

Braïda and Hiberty confirmed and expanded the previous conclusion in a comprehensive survey of first- and second-row dimer radical cations.[17] The investigation also covered 10 of the most widely used DFT functionals. In the study they found that the BHandHLYP method produced surprisingly accurate dissociation energies, but as UHF gave severely underestimated energies, the success of BHandHLYP was attributed to error cancellation. A recent study of $(H_2O)_2^{\bullet+}$ by Sodupe et al. included an excellent theoretical treatment of the failing.[18] The authors concluded that DFT overestimates the self-interaction part of the energy due to its delocalized electron hole. HF-based methods, on the other hand, treat the self-interaction exactly and are thus free from this particular problem. The $H_2^{\bullet+}$ and $He_2^{\bullet+}$ systems were recently reexamined in a study by Chermett et al.,[19] where they showed that the erroneous dissociation energies can be compensated for by a simple a posteriori correction. As this is a post-optimization correction, however, it will not enable correct geometries based on flawed wave functions.

Finally, Sastry et al. revisited the failing in a study of the hypersurface of $C_4H_6^{\bullet+}$, where they located the transition structure for the interconversion of the syn and anti rotamers of butadiene radical cation.[20] As a rotation around the central bond would transform one of the rotamers to the first exited state of the other rotamer, this is a state-symmetry-forbidden process in C_2 symmetry (see Figure 1). The transition structure must therefore localize spin and charge to one of the vinylic moieties in an asymmetric transition structure, so the coefficients in the other moiety can change signs.

10.1021/jp011336d CCC: $20.00
Published on Web 08/02/2001

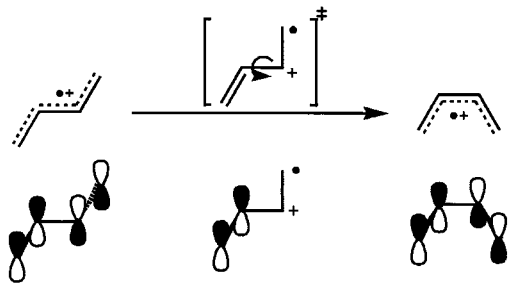

Figure 1. Singly occupied MO (SOMO) of *anti*- and *syn*-butadiene radical cation, with localized transition structure necessary for interconversion.

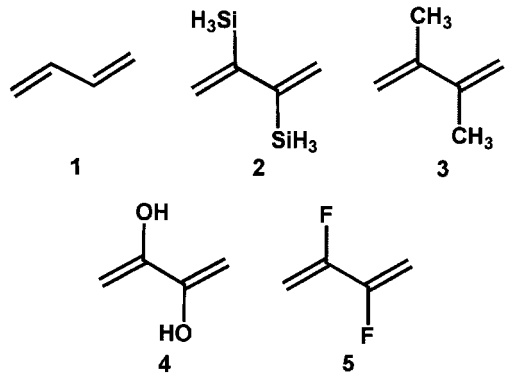

Figure 2. Butadiene radical cations included in this study.

Consequently, DFT performs poorly when modeling transition structures such as that, optimizing toward a C_2 symmetric structure instead of the correct asymmetric one. Indeed, the authors found that the BLYP and B3LYP functionals failed to locate the transition structure altogether, and only by utilizing the BHandHLYP functional could a transition structure be found. The authors concluded that it is impossible to correctly model these transition structures with DFT methods unless a significant admixture of Hartree−Fock exchange density is included.

In our work on conjugation in hydrocarbon radical cations,[21] we found that DFT correctly represented transition structures for butadiene radical cations when the hydrogens at C2 and C3 were substituted with silicon. It is not clear why the asymmetric transition structure could be located in this case but not that of the 1,3-butadiene radical cation or any of the other systems mentioned above, since a symmetry breaking is necessary in all cases. The origin of this must be the substitution, which prompted us to further investigate the effect of substitution and symmetry on the success, or lack thereof, when the most common DFT functionals are used.

This paper presents a theoretical study of the transition structures for rotamer interconversions of several symmetric 2,3-disubstituted butadiene radical cations (see Figure 2). In particular, we will investigate the following questions: (i) Can DFT overcome the overestimation of delocalization in order to give a C_1 symmetric transition structure? (ii) If so, what is the quality of the DFT result? (iii) What is the role of atomic versus electronic symmetry in the phenomenon described above? Given the problems associated with locating the asymmetric transition structures, we will also discuss the techniques that can be used in detail.

2. Computational Methodology

All calculations were performed with the Gaussian 98 program package,[22] running on SGI Origin2000 and Origin3000 machines at the High-Performance Computing Complex at the University of Notre Dame. Abbreviations used throughout this paper follow the ones used in Gaussian 98. Pure DFT calculations were carried out with the gradient-corrected exchange functional of Becke[23] combined with the correlation functional of Lee, Yang, and Par (BLYP).[24] Hybrid DFT calculations utilized Becke's three-parameter[25] (B3) and half-and-half (BHandH) exchange functionals[26] together with the LYP correlation functional. The B3LYP functional consists of a 20% admixture of Hartree−Fock exchange density, while the BHandHLYP functional incorporates 50% Hartree−Fock exchange density.[26] Complete active space (CASSCF) calculations were carried out with an active space consisting of three electrons in four active orbitals [CASSCF(3,4)] corresponding to the bonding π orbitals and their anti-bonding counterparts. In a few cases the orbital energies tended to fluctuate and therefore a larger active space was utilized; in all cases five electrons in six active orbitals. Conical intersections were located by the state-averaged CASSCF method.[27,28] Ab initio calculations normally used the unrestricted Hartree−Fock (UHF) formalism, followed by single point calculations by the accurate but very computationally demanding quadratic configuration interaction (QCI) method[29] with single, double, and triple excitations [QCISD(T)]. In a few systems, full QCISD optimizations, followed by single point QCISD(T) calculations, were performed. The double-ζ basis set 6-31G* developed by Pople and co-workers was used throughout the investigation.

Stationary points were, except where noted, located and characterized by vibrational analysis to ensure that all species had the correct number of eigenvalues. All relative energies reported were also zero-point-corrected. The one imaginary harmonic frequency of the transition structures was animated with MOLDEN[30] to verify that the optimized stationary point corresponds to the transition structure of the desired reaction. The stationary point wave functions were also checked for spin contamination by evaluation of the $\langle S^2 \rangle$ values. For BLYP and B3LYP calculations, $\langle S^2 \rangle$ before annihilation was generally between 0.75 and 0.76, the only exception being **ts-4**$^{\bullet+}$(B3LYP), which had a $\langle S^2 \rangle$ value of 0.79. $\langle S^2 \rangle$ values for BHandHLYP and UHF wave functions for the located transition structures were good, ranging from 0.75 to 0.77. Wave functions for the minimum energy conformers, however, were severely spin-contaminated, with BHandHLYP $\langle S^2 \rangle$ values between 0.80 and 0.85, and UHF $\langle S^2 \rangle$ values between 0.92 and 1.06.

3. Results and Discussion

3.1. Unsubstituted Butadiene Radical Cation. The first system studied was the unsubstituted butadiene radical cation **1**$^{\bullet+}$, which was studied by Sastry and Bally in their original publication.[20] As **1**$^{\bullet+}$ is the most simple symmetric butadiene radical cation, we felt that the model nature of **1**$^{\bullet+}$ warranted a detailed discussion in the context of the substituted analogues. The results described below also functions as a template for further studies of larger, substituted butadiene radical cations.

The transition structure **ts-1**$^{\bullet+}$ was located by first performing a CASSCF(3,4) search for a conical intersection using a geometry with the dihedral C1−C2−C3−C4 (φ) set to 90°. This was done following the observation that the CASSCF ^{2}A/^{2}B crossing point should be as similar to **ts-1**$^{\bullet+}$ as possible, apart from the localization of spin and charge.[20] Indeed, the conical intersection is C_2-symmetric with $\varphi = 89.7°$, r(C1−C2) = r(C3−C4) = 1.38 Å, and one negative eigenvalue corresponding to an imaginary frequency of −381 cm^{-1}. Consecutive transition structure optimizations with UHF, QCISD, and BHandHLYP

TABLE 1: Summary of Pertinent Geometry Parameters for *syn-* → *anti*-Butadiene Interconversion Transition States

	1$^{\bullet+}$				**2**$^{\bullet+}$				**3**$^{\bullet+}$			
parameter	*r*(C1−C2)	*r*(C2− C3)	*r*(C3− C4)	φ	*r*(C1−C2)	*r*(C2−C3)	*r*(C3−C4)	φ	*r*(C1−C2)	*r*(C2−C3)	*r*(C3−C4)	φ
UHF	1.32	1.47	1.41	92.5	1.33	1.43	1.39	84.1	1.32	1.49	1.42	88.9
QCISD	1.34	1.46	1.42	89.8	a	a	a	a	a	a	a	a
BHand-HLYP	1.32	1.45	1.41	90.3	1.33	1.43	1.39	85.5	a	a	a	a
B3LYP	b	b	b	b	1.34	1.44	1.39	93.7	b	b	b	b
BLYP	b	b	b	b	1.34	1.45	1.39	102.1	b	b	b	b

	4$^{\bullet+}$				**5**$^{\bullet+}$			
parameter	*r*(C1−C2)	*r*(C2− C3)	*r*(C3− C4)	φ	*r*(C1−C2)	*r*(C2−C3)	*r*(C3−C4)	φ
UHF	1.31	1.50	1.42	90.5	1.31	1.49	1.41	91.1
QCISD	1.33	1.49	1.42	88.5	a	a	a	a
BHand-HLYP	1.32	1.49	1.41	87.3	1.31	1.48	1.41	89.2
B3LYP	1.34	1.49	1.4 1	75.0	b	b	b	b
BLYP	b	b	b	b	b	b	b	b

[a] Structure not located. [b] Structure converged to C_2 symmetry. Bond lengths are in Angströms; dihedral angles are in degrees.

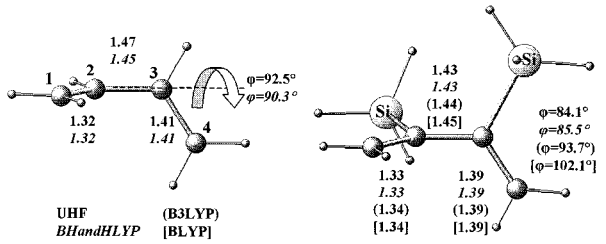

Figure 3. Stationary points **ts-1**$^{\bullet+}$ and **ts-2**$^{\bullet+}$ with pertinent geometrical parameters. Bond lengths are in Angströms; dihedral angles are in degrees.

calculations all gave a stationary point with one negative eigenvalue corresponding to rotation around the central bond, identifying it as **ts-1**$^{\bullet+}$. Pertinent geometrical parameters are summarized in Figure 3 as well as in Table 1. As can be seen in Figure 3, **ts-1**$^{\bullet+}$ is asymmetric with spin and charge localized to one of the π bonds, resulting in a lower electron density and consequently a longer C−C distance compared to the delocalized *anti*-**1**$^{\bullet+}$. The barrier to rotation was calculated as 29.4, 29.3, and 28.1 kcal/mol at the QCISD(T)/UHF, BHandHLYP, and QCISD(T)/QCISD levels, respectively.

Transition structure optimizations with B3LYP or BLYP, however, both optimized toward C_2-symmetric structures, at which point the negative eigenvalues disappeared and the transition structure optimization halted. Investigation of the B3LYP optimization revealed that φ progressed from 92.4° to >112°, which explains the disappearance of the negative eigenvalue. The failure of DFT to retain a localized asymmetric structure reaffirms the findings of Bally and Sastry.

3.2. (2,3-Disilyl)butadiene Radical Cation. B3LYP optimization of 2,3-disilylbutadiene radical cation (**2**$^{\bullet+}$) with φ set to 90°, followed by a transition structure optimization, gave a stationary point with one negative eigenvalue. Frequency calculations found that the negative eigenvalue corresponded to rotation around the central bond, and IRC calculations confirmed that the transition structure was indeed the correct one. **Ts-2**$^{\bullet+}$(B3LYP) is asymmetric (see Figure 3), with φ = 93.7°, *r*(C1−C2) = 1.34 Å, *r*(C3−C4) = 1.38 Å, and a relative energy 7.7 kcal/mol higher than that of the minimum-energy structure *anti*-**2**$^{\bullet+}$(B3LYP). **Ts-2**$^{\bullet+}$(BLYP) was also characterized, locating an asymmetric stationary point 5.7 kcal/mol higher than that of *anti*-**2**$^{\bullet+}$(BLYP). By use of **ts-2**$^{\bullet+}$(B3LYP) as a starting point, **ts-2**$^{\bullet+}$(UHF) and **ts-2**$^{\bullet+}$(BHandHLYP) were eventually located, with activation energies of 9.5 and 11.9 kcal/mol, respectively.

As **ts-2**$^{\bullet+}$ is selectively stabilized over *anti*-**2**$^{\bullet+}$ due to the orthogonal orbital geometry necessary for the β-silicon effect,[31] this would explain the lowered activation energy encountered for **2**$^{\bullet+}$ as compared to **1**$^{\bullet+}$. It was theorized that this stabilization overcomes the DFT overestimation of delocalization, providing a transition structure that is qualitatively correct. To test this hypothesis, other 2,3-(X,X)-disubstituted butadiene radical cations (X = -CH_3, -OH, and -F, labeled **3**$^{\bullet+}$, **4**$^{\bullet+}$, and **5**$^{\bullet+}$, respectively) were investigated (see Figure 2).[32] It was reasoned that the transition structure energies should be lowered by the substituents in the order -H < -F < -CH_3 < -OH < -SiH_3, as judged by their σ^+ values. It should be noted that while there is no orbital orthogonality requirement, as is the case for **2**$^{\bullet+}$, the lowering of the activation energy is achieved through an offsetting of the energy lost when conjugation is disrupted.

The search for transition structures followed the same procedure as outlined for **1**$^{\bullet+}$. As often is the case with radical ions, however, there is no general recipe for success, and despite the small size of the system, the localization of the transition structure can be slow and tedious.

3.3. (2,3-Dimethyl)butadiene Radical Cation. No conical intersection could be found for **3**$^{\bullet+}$. After an initial optimization of the carbon skeleton, the optimization settled into a pattern where the C−H bond lengths would cycle through values between 1.04 and 1.16 Å. Attempts initiated from different starting geometries all ended in the same oscillatory mode. By submission of several of the oscillating geometries to UHF frequency calculations, a structure with one negative eigenvalue was eventually located. A UHF transition structure optimization from this geometry led to a transition structure 17.8 kcal/mol higher than the minimum-energy conformer *syn*-**3**$^{\bullet+}$(UHF). **Ts-3**$^{\bullet+}$(UHF) is an asymmetric structure with φ = 88.9°, *r*(C1−C2) = 1.32 Å, and *r*(C3−C4) = 1.42 Å. It has one imaginary harmonic frequency corresponding to the correct vibration. Attempts to generate a starting point for BHandHLYP optimizations failed as no structures with less than three negative eigenvalues were generated. While one of the negative eigenvalues corresponded to the correct rotation, the remaining two negative eigenvalues corresponded to rotation around the C−CH_3 bonds. Attempts to eliminate the superfluous negative eigenvalues, either by manual rotation of the C−CH_3 bonds or reoptimization with the all atoms except the -CH_3 atoms frozen, also eliminated the desired negative eigenvalue. B3LYP and

TABLE 2: Summary of Activation Energies for Interconversion of *anti*- → *syn*-Butadiene Radical Cations

	$1^{\bullet+}$	$2^{\bullet+}$	$3^{\bullet+}$	$4^{\bullet+}$	$5^{\bullet+}$
UHF	28.2	13.7	20.6	12.0	28.2
QCISD(T)/UHF	29.4	9.9	18.5	8.9	25.7
QCISD(T)/QCISD	28.1	a	a	9.0	a
BHandHLYP	29.3	11.0	a	7.5	28.3
B3LYP	b	7.7	b	8.7	b
BLYP	b	5.7	b	b	b

[a] Structure not located. [b] Structure converged to C_2 symmetry. Activation energies are given in kilocalories per mole.

BLYP, however, fared better. While frequency calculations of the **ts-3**$^{\bullet+}$(UHF) geometry also gave undesired negative eigenvalues corresponding to methyl rotation, reoptimization with all other atoms frozen gave starting points with only the one desired negative eigenvalue. Transition structure optimizations from these starting points failed, however, when both methods optimized toward an asymmetric structure, parallel to the behavior encountered when locating **ts-1**$^{\bullet+}$.

3.4. (2,3-Dihydroxy)butadiene Radical Cation. Similar to **3**$^{\bullet+}$, conical intersection optimizations of **4**$^{\bullet+}$ ended in an oscillatory pattern where one of the C−O bonds rotated back and forth. By submission of several of the oscillating geometries to BHandHLYP frequency calculations, a structure with one negative eigenvalue was eventually located. Transition structure optimizations from this structure lead to **ts-4**$^{\bullet+}$(BHandHLYP). **Ts-4**$^{\bullet+}$(BHandHLYP) is an asymmetric structure with $\varphi = 87.3^\circ$, r(C1−C2) = 1.32 Å, and r(C3−C4) = 1.41 Å (see Table 2) and an energy 7.5 kcal/mol higher than the minimum-energy structure *anti*-**4**$^{\bullet+}$(BHandHLYP).[33] Interestingly, UHF, B3LYP, and BLYP frequency calculations of **ts-4**$^{\bullet+}$(BHandHLYP) all gave two negative eigenvalues, where one corresponded to the desired motion and the other corresponded to a C−O bond rotation. Reoptimizing **ts-4**$^{\bullet+}$(BHandHLYP) with all carbons frozen eliminated the second negative eigenvalue, and consecutive transition structure optimizations with UHF and B3LYP led to **ts-4**$^{\bullet+}$(UHF) and **ts-4**$^{\bullet+}$(B3LYP). Pertinent geometrical properties can be found in Table 1. The barrier to rotation was calculated as 9.9 and 8.7 kcal/mol, respectively. BLYP calculations, on the other hand, failed. BLYP frequency calculations of **ts-4**$^{\bullet+}$(B3LYP) geometry yielded force constants with one negative eigenvalue, but transition structure optimizations failed when the negative eigenvalue disappeared at $\varphi = 68.5^\circ$. Of note is that **4**$^{\bullet+}$(BLYP) was still asymmetric when it failed, with r(C1−C2) = 1.36 Å and r(C3−C4) = 1.39 Å. As these values are significantly closer to C_2 symmetry than the starting point with r(C1−C2) = 1.32 Å and r(C3−C4) = 1.41 Å, however, it is reasonable to believe that **4**$^{\bullet+}$(BLYP) would eventually have achieved C_2 symmetry had the optimization continued.

To better evaluate the B3LYP transition structure compared to an accurate transition structure, a QCISD(T)/QCISD transition structure optimization was performed, with geometry and force constants read from a **ts-4**$^{\bullet+}$(B3LYP) frequency calculation.[34] **Ts-4**$^{\bullet+}$(QCISD) is a C_1-symmetric structure with $\varphi = 88.5^\circ$, r(C1−C2) = 1.33 Å, and r(C3−C4) = 1.42 Å. The non-zero-point-corrected activation energy was calculated to be 9.0 kcal/mol. For comparison purposes, the non-zero-point-corrected activation energies from the QCISD(T)/UHF, BHandHLYP, and B3LYP methods were calculated to be 8.9, 7.1, and 9.4 kcal/mol, respectively. Another measure of the accuracy of the **ts-4**$^{\bullet+}$(B3LYP) geometry is comparing QCISD(T) single point calculations of **ts-4**$^{\bullet+}$(B3LYP) and **ts-4**$^{\bullet+}$(QCISD). By doing so, **ts-4**$^{\bullet+}$(B3LYP) was found to be 2.4 kcal/mol higher than **ts-4**$^{\bullet+}$(QCISD).

3.5. (2,3-Difluoro)butadiene Radical Cation. The conical intersection for the last species studied, **5**$^{\bullet+}$, was fairly easily located at $\varphi = 87.1^\circ$. As expected, it is C_2-symmetric with r(C1−C2) = r(C3−C4) = 1.37 Å. Starting from the conical intersection, **ts-5**$^{\bullet+}$(UHF) and **ts-5**$^{\bullet+}$(BHandHLYP) were located at $\varphi = 91.1^\circ$ and $\varphi = 89.2^\circ$, respectively. Both are asymmetric structures with r(C1−C2) = 1.31 Å, r(C3−C4) = 1.41 Å, and one imaginary harmonic frequency corresponding to the correct dihedral. The barrier to rotation was calculated as 28.2 and 28.3 kcal/mol, respectively. Starting geometries for B3LYP and BLYP transition structure optimizations were generated from **ts-5**$^{\bullet+}$(BHandHLYP). BLYP failed in the manner described earlier, going to a C_2-symmetric structure with r(C1−C2) = r(C3−C4) = 1.37 Å, losing its negative eigenvalue at $\varphi = 95.5^\circ$. The B3LYP optimization, while also going to a C_2-symmetric structure with r(C1−C2) = r(C3−C4) = 1.37 Å, optimized φ in the other direction, and lost its negative eigenvalue at $\varphi = 44.5^\circ$. As all other failures optimized toward the minimum-energy conformer, the B3LYP results are surprising. Despite several attempts to rationalize the disparate behaviors of the B3LYP and BLYP methods, no solid reason was apparent, and so once again the flatness of the hypersurface appeared to be the culprit.

4. Discussion and Conclusions

The results of this investigation are summarized in Table 2. Overall, HF and BHandHLYP methods are able to locate the desired transition structures, the only exception being **3**$^{\bullet+}$ with BHandHLYP. This is most likely an isolated case, however, and not indicative of an underlying fundamental problem. For BLYP and B3LYP, the systems studied can be divided broadly into two categories. In category I, composed of **1**$^{\bullet+}$, **3**$^{\bullet+}$, and **5**$^{\bullet+}$, DFT wave functions converge toward a symmetric, delocalized solution. In category II, composed of **2**$^{\bullet+}$ and **4**$^{\bullet+}$, DFT wave functions correctly converge to the localized solution. It can also be seen that, when found, the calculated activation energies correspond quite well to each other, well within the margin of error accepted for other systems.[35] In particular, QCISD(T) single point calculations found that the **ts-4**$^{\bullet+}$(B3LYP) geometry only deviated 2.4 kcal/mol from the high-level **ts-4**$^{\bullet+}$(QCISD) geometry.

In answer to the questions posed before, it is clear that DFT can overcome the overestimation of delocalization in order to obtain a asymmetric structure. Furthermore, when the results in categories I and II are compared, a trend is apparent. In category I, where B3LYP and BLYP methods converge to C_2-symmetric solutions, activation energies are calculated to be >18 kcal/mol. In category II, where DFT methods are more successful, activation energies are calculated to be substantially lower, between 5.7 and 11.0 kcal/mol. Although the dataset is fairly limited, the amount of stabilization needed for pure DFT to overcome overestimation of the delocalized solution is found to be ∼20 kcal/mol compared to the unsubstituted case.

It is also clear that symmetry is not inherently a problem. This is most apparent in the location of the asymmetric **ts-2**$^{\bullet+}$(B3LYP), where B3LYP breaks the symmetry of the starting geometry. Instead of molecular symmetry, however, one must consider what might be called electronic symmetry. Asymmetric compounds such as 2-fluorobutadiene radical cation or 2-fluoro-3-methylbutadiene radical cation have substituents with fairly similar σ^+ values and are thus likely to encounter the same problems with overestimation of delocalization. Preliminary calculations on the 2-fluorobutadiene radical cation systems indicate that this is, indeed, the case.

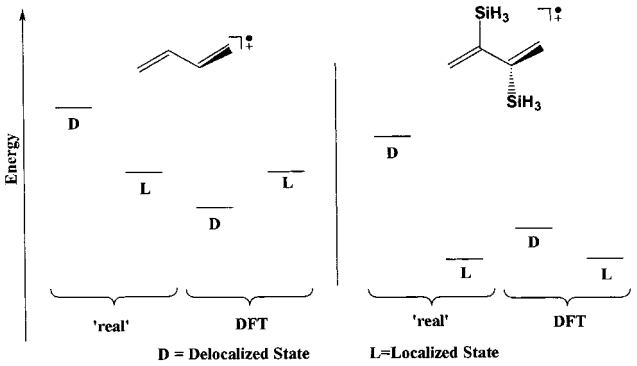

Figure 4. Two-state model for **ts-1**$^{\bullet+}$ and **ts-2**$^{\bullet+}$ of delocalized state vs localized state.

More importantly, we have found that the error encountered is binary in nature. When the DFT transition structure optimization fails, it fails completely. Where it works, however, the properties of the transition structure are correctly modeled even by pure DFT. This is rationalized by a two-state model (see Figure 4). When performing the optimization, the system can converge to either a delocalized (symmetric) state D or a localized (asymmetric) state L. With a Hartree−Fock-based method, L is the lower energy state, and the solution found will be the correct, localized one. With a DFT method, however, the overestimation of delocalization lowers the D state so that it is now the lower energy state. The DFT method will therefore optimize toward the D state, and eventually fail, as there is no delocalized transition state.

When a stabilizing substituent such as the silyl in **2**$^{\bullet+}$ is introduced, the L state is selectively stabilized versus the D state. For Hartree−Fock methods this does not matter, as the L state is already the lower one. For DFT methods, this selective stabilization might be enough to overcome the bias toward the D state. If so, the absolute energy of the L state should not be influenced by the D state, as there is no delocalization to overestimate. DFT would therefore not only find the L state solution, but it would also describe it quantitatively correctly. It should also be noted that this model is consistent with the theoretical treatment provided by Sodupe et al.,[18] provided that it is only applied to the D state.

Acknowledgment. We gratefully acknowledge financial support of this research by the Volkswagen Foundation (I/72 647) and the National Science Foundation (CHE97-33050) and allocation of computational resources by the OIT at the University of Notre Dame. J.O. thanks the Department of Chemistry and Biochemistry for funding provided through the Reilly fellowship. We also thank Dr. Thomas Bally for his assistance in explaining the pitfalls of computational organic radical cation chemistry.

Supporting Information Available: Tables of gas-phase coordinates, energies, QCISD(T) single-point energies, S^2 values, and negative frequencies for all stationary points, geometries and energies of all conical intersections. This material is available free of charge via the Internet at http://pubs.acs.org.

References and Notes

(1) Koch, W.; Holthausen, M. C. *A Chemist's Guide to Density Functional Theory;* Wiley−VCH: Weinheim, Germany, and Chichester, U.K., 2000.

(2) Bally, T.; Borden, W. T. *Rev. Comput. Chem.* **1999**, *13*, 1.

(3) (a) Labanowski, J.; Andzelm, J. *Density Functional Methods in Chemistry*; Springer-Verlag: New York, 1991. (b) Ziegler, T. *Chem. Rev.* **1991**, *91*, 651. (c) Wiest, O.; Black, K. A.; Houk, K. N. *J. Am. Chem. Soc.* **1994**, *116*, 10336. (d) Truong, T. N.; Duncan, W. T.; Bell, R. L. *ACS Symp. Ser*. **1996**, *629*, 85. (e) Durant, J. L. *Chem. Phys. Lett*. **1996**, *256*, 595. (f) Truhlar, D. G. *Faraday Discuss.* **1998**, *110*, 362.

(4) Curtiss, L. A.; Raghavachari, K.; Redfern, P. C.; Pople, J. A. *J. Chem. Phys.* **1997**, *106*, 1063.

(5) Bally, T.; Bernhard, S.; Matzinger, S.; Truttmann, L.; Zhu, Z.; Roulin, J.; Marcinek, A.; Gebicki, J.; Williams, F.; Chen, G.; Roth, D.; Herbertz, T. *Chem. Eur. J.* **2000**, *6*, 849.

(6) Merril, G. N.; Kass, S. R. *J. Phys. Chem.* **1996**, *100*, 17465.

(7) Niu, S.; Hall, B. M.; *Chem. Rev.* **2000**, *100*, 353.

(8) (a) Karpfen, A.; Choi, C. H.; Kertesz, M. *J. Phys. Chem. A* **1997**, *101*, 7426−7433 (b) Karpfen, A. *J. Phys. Chem. A* **1999**, *103*, 2821.

(9) Choi, C. H.; Kertesz, M. *J. Phys. Chem. A* **1997**, *101*, 3823.

(10) (a) Ma, N. L.; Smith, B. J.; Radom, L. *Chem. Phys. Lett.* **1992**, *193*, 386. (b) Nobes, R. H.; Moncrieff, D.; Wong, M. W.; Radom, L.; Gill, P. M. W.; Pople, J. A. *Chem. Phys. Lett.* **1991**, *182*, 216.

(11) Noodleman, L.; Post, D.; Baerends, E. *J. Chem. Phys.* **1982**, *64*, 159.

(12) Barnett, R. N.; Landman, U. *J. Phys. Chem.* **1995**, *99*, 17305.

(13) Hrusak, J.; Friedrichs, H.; Schwarz, H.; Razafinjanahary, H.; Chermette, H. *J. Phys. Chem.* **1996**, *100*, 100.

(14) Hiberty, P. C. In *Modern Electronic Structure Theory and Applications in Organic Chemistry*; Davidson, E. R., Ed.; World Scientific: River Edge, NJ, 1997; p 289.

(15) Hrouda, V.; Roeselová, M.; Bally, T. *J. Phys. Chem. A* **1997**, *101*, 3925.

(16) Bally, T.; Sastry, G. N. *J. Phys. Chem. A* **1997**, *101*, 7923.

(17) Braïda, B.; Hiberty, P. C. *J. Phys. Chem. A* **1998,** *102*, 7872.

(18) Sodupe, M.; Bertran, J.; Rodriguez-Santiago, L.; Baerends, E. J. *J. Phys. Chem. A* **1999,** *103*, 166.

(19) Chermette, H.; Ciofini, I.; Mariotti, F.; Daul, C. *J. Chem. Phys.* **2001**, *114*, 1447.

(20) Sastry, G. N.; Bally, T.; Hrouda, V.; Carsky, P. *J. Am. Chem. Soc.* **1998**, *120*, 9323.

(21) Oxgaard, J.; Wiest, O. To be published.

(22) Frisch, M. J.; Trucks, G. W.; Schlegel, H. B.; Scuseria, G. E.; Robb, M. A.; Cheeseman, J. R.; Zakrzewski, V. G.; Montgomery, J. A., Jr.; Stratmann, R. E.; Burant, J. C.; Dapprich, S.; Millam, J. M.; Daniels, A. D.; Kudin, K. N.; Strain, M. C.; Farkas, O.; Tomasi, J.; Barone, V.; Cossi, M.; Cammi, R.; Mennucci, B.; Pomelli, C.; Adamo, C.; Clifford, S.; Ochterski, J.; Petersson, G. A.; Ayala, P. Y.; Cui, Q.; Morokuma, K.; Malick, D. K.; Rabuck, A. D.; Raghavachari, K.; Foresman, J. B.; Cioslowski, J.; Ortiz, J. V.; Stefanov, B. B.; Liu, G.; Liashenko, A.; Piskorz, P.; Komaromi, I.; Gomperts, R.; Martin, R. L.; Fox, D. J.; Keith, T.; Al-Laham, M. A.; Peng, C. Y.; Nanayakkara, A.; Gonzalez, C.; Challacombe, M.; Gill, P. M. W.; Johnson, B. G.; Chen, W.; Wong, M. W.; Andres, J. L.; Head-Gordon, M.; Replogle, E. S.; Pople, J. A. *Gaussian 98*, revision A.9; Gaussian, Inc.: Pittsburgh, PA, 1998.

(23) Becke, A. D. *Phys. Rev. A* **1988**, *37*, 3098.

(24) Lee, C.; Yang, W.; Parr, R. G. *Phys. Rev. B* **1988**, *37*, 785.

(25) Becke, A. D. *J. Chem. Phys.* **1993**, *98*, 5648.

(26) These are *not* the same functionals as the half-and-half functionals proposed by Becke (*J. Chem. Phys*. **1993**, *98*, 1372), instead implemented by Gaussian 98 as BHandHLYP: $0.5E_X^{HF} + 0.5E_X^{LSDA} + 0.5E_X^{Becke88} + 0.5E_C^{LYP}$.

(27) Ragazos, I. N.; Robb, M. A.; Bernardi, F.; Olivucci, M. *Chem. Phys. Lett.* **1992**, *197*, 217.

(28) Bearpark, M. J.; Robb, M. A.; Schlegel, H. B. *Chem. Phys. Lett.* **1994**, *223*, 269.

(29) Pople, J. A.; Head-Gordon, M.; Raghavachari, K. *J. Chem. Phys.* **1987**, *87*, 3700.

(30) MOLDEN version 3.5, written by G. Schaftenaar (Netherlands). For details of this program, see the URL http://www.caos.kun.nl/∼schaft/molden.

(31) Lambert, J. B.; Zhao, Y.; Emblidge, R. W.; Salvador, L. A.; Liu, X.; So, J.; Chelius, E. C. *Acc. Chem. Res.* **1999**, *32*, 183.

(32) We also investigated the 2,3-diamino-substituted butadiene radical cation. A conical intersection could be located at $\varphi = 69.9^{\circ}$, but all subsequent attempts to locate an area with negative eigenvalues were unsuccessful, presumably to the flatness of the hypersurface.

(33) It should be noted that the minimum energy conformer is the *syn*-**5**$^{\bullet+}$, 6.9 kcal/mol lower in energy than *anti*-**5**$^{\bullet+}$, due to hydrogen bonding in the syn geometry. As the hydrogen bond is absent in the transition structure, we felt that energy comparisons were best made to the anti conformer.

(34) Similar transition state optimizations were initiated from **ts-4**$^{\bullet+}$-(UHF) and **ts-4**$^{+}$(BHandHLYP) as well but failed when the SCF wave function would not converge, even with the convergence criteria set as low as 10^{-4} hartrees.

(35) See for example; Lynch, B. J.; Fast, P. L.; Harris, M.; Truhlar, D. G. *J. Phys. Chem. A* **2000**, *104*, 21.